



PVD surface treatment of heat-treated cast aluminium alloys

T. Tański *, L.A. Dobrzański, M. Wiśniowski, T. Linek, R. Szklarek

Institute of Engineering Materials and Biomaterials, Faculty of Mechanical Engineering,
Silesian University of Technology, ul. Konarskiego 18a, 44-100 Gliwice, Poland

* Corresponding e-mail address: tomasz.tanski@polsl.pl

ABSTRACT

Purpose: Main purpose of the paper is results share of AlSi9Cu and AlSi9Cu4 cast aluminium alloys treatment investigation. Processing was performed using CAE-PVD method in order to obtain gradient coatings.

Design/methodology/approach: CAE-PVD method was used to obtain gradient coatings on AlSi9Cu and AlSi9Cu4 cast aluminium alloys after heat treatment. Investigation of resulting material was performed using SEM, TEM, GDOS, ball-on-disk wear resistance test and microhardness test.

Findings: The investigations presented in this paper reveal that it was possible to successfully deposit Cr/CrN/CrN, Cr/CrN/TiN, and Ti/Ti(C,N)/(Ti,Al)N nano-crystalline coatings on Al-Si-Cu aluminium substrate using CAE-PVD method. Investigations of the coatings reveal a microstructure that adhere tightly to the aluminium substrate without any visible delamination but with visible transition zone between the investigated layers and the substrate material.

Research limitations/implications: There is need for further research activity in field of nanocomposite films and coatings that should concentrate on following problems: controlled grain size of coatings/films, development of hybrid coatings with unique physical and functional properties, e.g. nanophase biomaterials.

Practical implications: Better understanding of mechanisms that proceed during CAE-PVD treatment of AlSi9Cu and AlSi9Cu4 cast aluminium alloys. Creation of material, that, thanks to the treatment, can be coated with layer characterized by gradient chemical composition with unique physical and functional properties (e.g. higher microhardness or corrosion resistance, lower friction coefficient, etc.) that can be successfully applied within aerospace and automotive industry or even on field of biomedical applications with use of nanophase biomaterials or nano-crystalline amorphous materials.

Originality/value: Cr/CrN/CrN, Cr/CrN/TiN, and Ti/Ti(C,N)/(Ti,Al)N nano-crystalline coatings were deposited on Al-Si-Cu aluminium substrate. They are characterized by visible transition zone (gradient) between the investigated layers and the substrate material.

Keywords: CAE-PVD; AlSi9Cu; AlSi9Cu4; SEM; TEM; GDOS; Ball-on-disc; Wear resistance

Reference to this paper should be given in the following way:

T. Tański, L.A. Dobrzański, M. Wiśniowski, T. Linek, R. Szklarek, PVD surface treatment of heat-treated cast aluminium alloys, Archives of Materials Science and Engineering 79/2 (2016) 79-88.

MATERIALS MANUFACTURING AND PROCESSING

1. Introduction

In recent years, there has been growing interest in light metals and especially in materials with low density and relatively high strength properties. This group of materials includes, in particular, aluminium, magnesium, and their alloys [1-5]. Non-ferrous alloys find applications in the automobile and aviation industries. The big popularity of the aluminium and magnesium alloys in these branches of industry is connected with their general functional properties, namely their low density, good mechanical properties, and very good machinability [1,2]. The deposition of hard coatings on material surfaces by PVD technology, among all methods to improve the mechanical properties of materials, is a rapidly evolving group of improving functionality technology. This technology makes it possible to modify the surface by shaping the physical and chemical properties. New operating characteristics of the commonly known non-ferrous alloys may be frequently obtained by depositing simple monolayer, multilayer, gradient, or nanocomposite coatings using the PVD methods. Among the surface-engineering techniques employed in the last two decades, gas and plasma nitriding, hard-coating PVD, and duplex treatments are the most popular methods reported in the literature. Hard coatings are usually chemically resistant at moderate temperature, provided they have the relevant thickness, are tight, and do not show the columnar structure. However, the majority of coatings deposited by the PVD and CVD processes have a high defect density in the form of pores and a columnar microstructure, which allows penetration of aggressive agents into the material [11-13]. Deposition of hard layers of nitrides, carbides, or oxides on the surface of engineering materials in the PVD processes is the most intensive direction of development for extending the lives of the functional elements [6-18]. Selection of the substrate material onto which the investigated coatings are deposited by the PVD technique in the presented project is not incidental either. Traditionally, automotive components and products used in the building and power industries should have, in addition to their special aesthetic features, high corrosion-, erosion-, and wear-resistance. Thin, hard PVD coatings on a soft substrate turn out to be an advantageous material combination from the material point of view [6-10]. The high mechanical properties, including hardness and strength of the nanocomposite coatings, are the result of hindering the movement of dislocations through the small grain and in the spaces between them, resulting in a loss of cohesion and incoherent deformation. This is the main concept in the achievement of good mechanical properties, including high

hardness of nanostructure coatings and high strength related to it, and particularly in the case of nanocomposite coatings, the increase and movement of dislocations is restricted. Another important issue is when the grain size is reduced to nanometre size, restricting the activity of dislocations as the causation of the material ductility [6,12,13]. According to the Hall-Petch equation, the strength properties of the material increase with the reductions of the grain size. In the case of the coatings deposited by the PVD process, the structures obtained with a grain size of ~ 10 nm achieve the maximum mechanical properties. Coatings of such structures present a very high hardness of > 40 GPa, ductility, and stability at high temperatures [12].

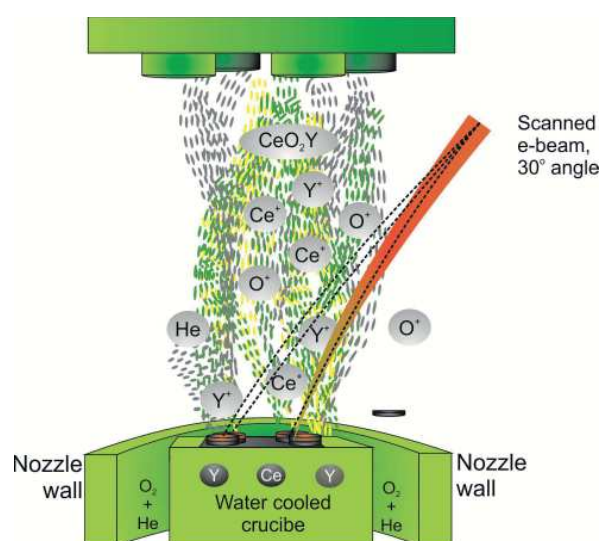


Fig. 1. Exemplary beam performance of PVD process

The aim of this work was to use the cathodic arc evaporation (CAE) PVD process to obtain the best possible hybrid coatings, consisting of a gradient with an intermediate layer, with a continuous change of one or more components in scope from the substrate to the surface top, as well as an outer coating on the surface of the cast aluminium alloys, in order to increase the low stiffness of the substrate material (Fig. 1). This article focuses on a very important surface engineering issue, namely, surface treatment using vacuum techniques of selected aluminium cast alloys. These alloys are currently recognised by materials science experts as future materials that combine low density and high strength. This improves their functional properties as well as provides the possibility of employing the finite element method (FEM) assessment of stress in the examined coatings. The key question here seems to be the provisioning of simultaneous development of both production technology

and processing of the light construction materials and technology of forming and protecting their surfaces, which will, in consequence, enable the maintenance of a balance between the modern substructure material and new generation coatings [2,16,17].

2. Materials and investigation procedure

Investigations were performed on samples made of AlSi9Cu and AlSi9Cu4 cast aluminium alloys after heat treatment (Table 1).

The applied method was implemented using a Dreva ARC400 device supplied by Vakuumentchnik, fitted with the electric arc cathodic evaporation method. The device is equipped with three separate sources of metal vapours. Samples in the form of discs 65 mm in diameter were used for PVD coatings containing pure target metals Cr and Ti as well as TiAl alloys, and were cooled with water. The coatings were deposited in a reactive N₂ atmosphere and an inert atmosphere of Ar, in order to generate a mixture of nitrides, as well as respectively, in an N₂ and C₂H₂ mixture, in order to obtain layers of carbo-nitrides. The gradient change of chemical composition concentration of the coating cross-section was achieved by changing the evaporation current on the arc sources or changing the proportion of reactive gas. The applied coating process conditions are presented in Table 2.

An SEM microscope was equipped with energy dispersive X-ray emission (EDX) to perform the chemical composition analysis presented in this paper.

Examinations of the thin foils microstructure and the phase identification were carried out on a JEOL 3010 transmission electron microscope (TEM) at an accelerating voltage of 300 kV using the selected area diffraction (SAD) method for phase investigations. The diffraction patterns from TEM were solved using dedicated computer software. The cross-sectional atomic composition of the samples

(coating and substrate) was obtained by using the glow discharge optical spectrometer GDOS-850 QDP supplied by Leco Instruments. The following working conditions of the Grimm-type glow discharge lamp spectrometer were fixed during the tests: a lamp inner diameter of 4 mm, lamp supply voltage of 1000 V, lamp current of 40 mA, and working pressure of 100 Pa.

Wear resistance investigations were performed using the ball-on-disk method. A tungsten carbide ball with a diameter of 3 mm was used as the counterpart. The tests were performed at room temperature for a defined time under the following test conditions: a load of Fn-5N, disk rotation of 200 rpm, wear radius of 2.5 mm, and shift rate of -0.05 m/s. The microhardness tests of the coatings were carried out with a Shimadzu DUH 202 ultra-microhardness tester. Measurements were made with 10 mN load to eliminate the influence of the substrate on the coating hardness. The measurement of the roughness of the surface of the obtained coatings was carried out using a Diavite Compact profilographometer from Asmeo Ag Company. The measurement length was Lc = 0.8 mm and the measurement accuracy was ± 0.02 µm.

Table 1.
Chemical composition of the investigated aluminium alloys

Type	Mass concentration of the elements, %				Rest
	Si	Fe	Cu	Mn	
AlSi9Cu	9.09	0.72	1.05	0.36	0.08
	Mg	Zn	Ti	Al	
	0.27	0.14	0.07	88.17	
Type	Mass concentration of the elements, %				Rest
	Si	Fe	Cu	Mn	
AlSi9Cu4	9.27	0.17	4.64	0.01	0.09
	Mg	Zn	Ti	Al.	
	0.28	0.05	0.09	85.4	

Table 2.
Deposition parameters of the investigated coatings

Coating parameters	Value for the Cr/CrN-gradient/CrN coating	Value for the Cr/CrN-gradient/TiN coating	Value for the Ti/Ti(C,N)-gradient/(Ti,Al)N coating
Base pressure [Pa]	5×10^{-3}	5×10^{-3}	5×10^{-3}
Working pressure [Pa]	1.0/1.4-2.3/2.2	1.0/1.4-2.3/2.2	0.9/1.1-1.9/2.8
Argon flow rate measurement, cm ³ /min	80*, 80**, 20***	80*, 80**, 20***	80*, 10**, 10***
Nitrogen flow rate measurement, cm ³ /min	0→250**, 250***	0→250**, 250***	0→225**, 0→350***
Acetylene flow rate measurement, cm ³ /min	-	-	140→0**
Substrate bias voltage, V	60*, 60**, 60***	60*, 60**, 100***	70*, 70**, 70***
Target current, A	60	60	60
Process temperature, °C	<150	<150	<150

3. Investigation results

The obtained solution-reinforced coatings of selected types, produced as a result of synthesis of unbalanced (metastable) phases, are characteristic of the high surface heterogeneity related to the occurrence of numerous micro-particles with different shapes and congealed droplets that fall out of the obtained layer during the deposition process, as well as hollows obtained as a result of drops falling out during the solidification process (Figs. 2-5).

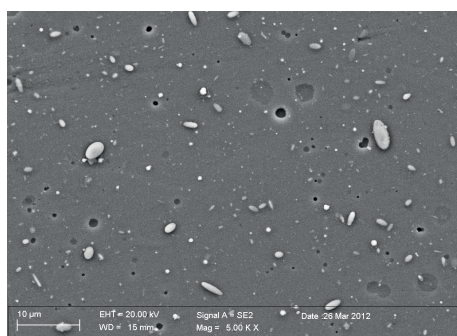


Fig. 2. Surface morphology of the Cr/CrN/CrN layer coated on the AlSi9Cu aluminium substrate

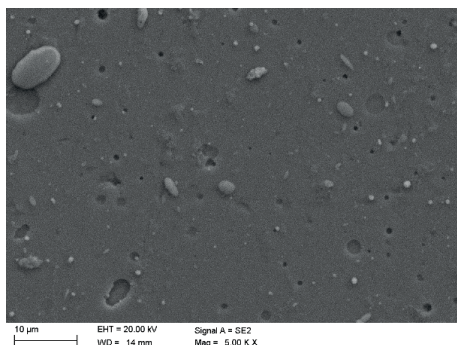


Fig. 3. Surface morphology of the Cr/CrN/TiN layer coated on the AlSi9Cu aluminium substrate

Among the coating surfaces investigated, the highest non-uniformity of the surface was obtained by the coating of the applied Ti/Ti(C,N)/(Ti,Al)N system, where numerous particles of the solidified vapour were found (Fig. 5). The lowest amount of solidified droplets of the vaporised metal was identified in the case of the Cr/CrN/TiN coating (Figs. 3 and 4) for both types of substrates. This is connected with the nature of the CAE method used for coating deposition. Depending on the process conditions, including the kinetic energy of the

drops sputtered into the metal substrate and the nature of the metal vapour source, the observed particles are clearly different in terms of shape and size. Moreover, it was also observed that characteristic cavities, formed as a result of droplets falling out after completion of the PVD process, are present on the surface of the obtained coatings.

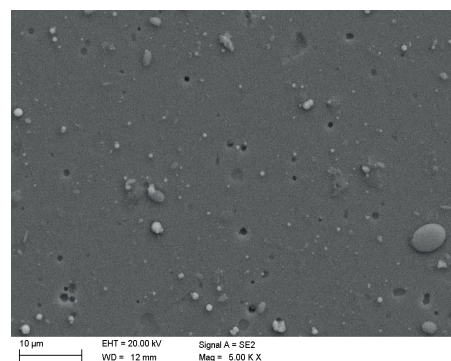


Fig. 4. Surface morphology of the Cr/CrN/TiN layer coated on the AlSi9Cu aluminium substrate

As a result of metallographic fracture investigations of samples made from aluminium alloys coated with the analysed coatings, performed using SEM, clear transition zones between the substrate and the coating were identified. The obtained coatings reveal a compact structure without visible delamination or defects; they are uniform and adhere tightly to each other as well as to the substrate (Figs. 6-8). Investigations of fractures confirm that shells of the type Ti/Ti(C,N)/(Ti,Al)N show a clearly layered structure with a clearly visible transition zone between the coating and the wear-resisting gradient coating, achieved by the appliance of separate sources of the metal vapour (Fig. 8).

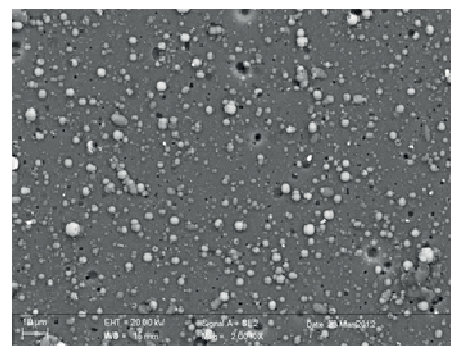


Fig. 5. Surface morphology of the Ti/Ti(C,N)/(Ti,Al)N layer coated on the AlSi9Cu aluminium substrate

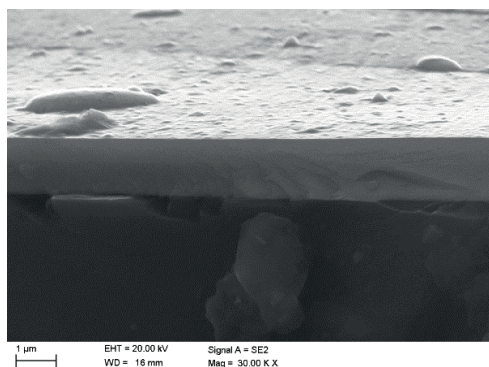


Fig. 6. Fracture of the Cr/CrN/CrN coating on the AlSi9Cu4 aluminium substrate

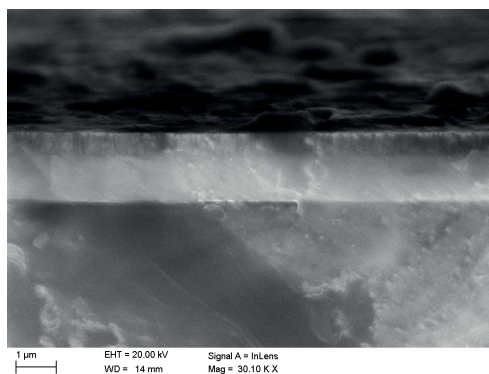


Fig. 7. Fracture of the Cr/CrN/TiN coating on the AlSi9Cu4 aluminium substrate

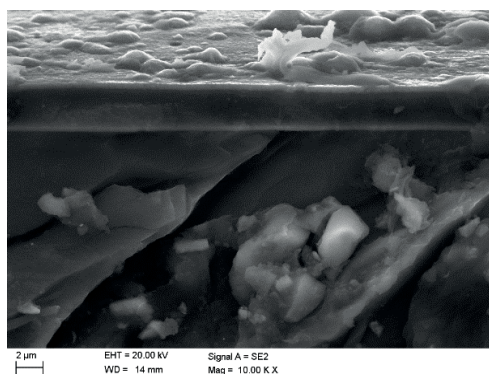


Fig. 8. Fracture of the Ti/Ti(C,N)/(Ti,Al)N coating on the AlSi9Cu4 aluminium substrate

In the case of the Cr/CrN/CrN coating, where are the same chemical elements in the gradient layer, only small differences on the cross-section structure have been found (Fig. 6).

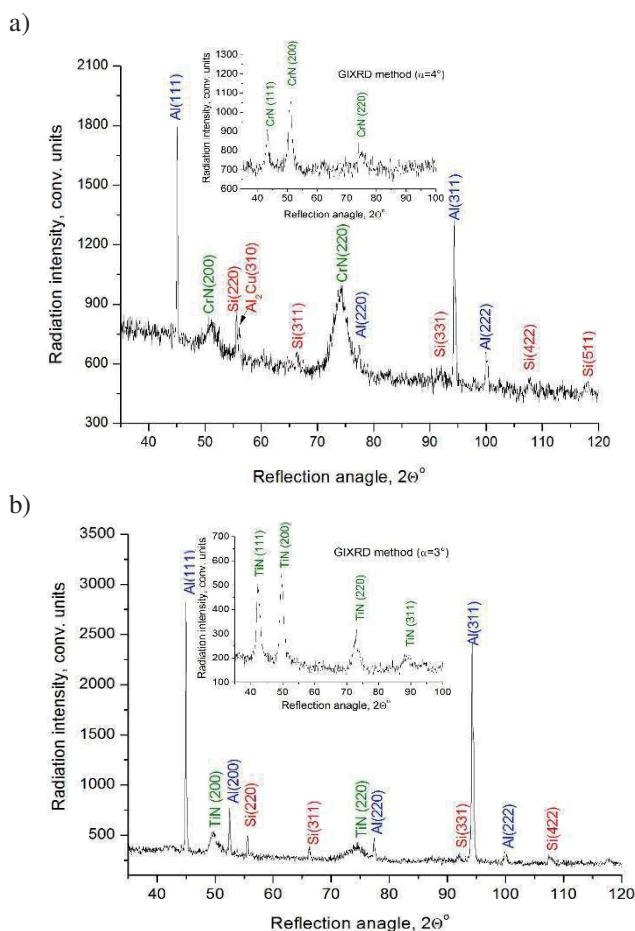


Fig. 9. X-ray diffraction pattern of: a) Cr/CrN/CrN coating deposited on the AlSi9Cu4 aluminium alloy, b) Cr/CrN/TiN coating deposited on the AlSi9Cu4 aluminium alloys obtained by Bragg-Brentano method and GIXRD method

Qualitative phase composition analysis carried out using the X-ray diffraction method has allowed to evaluate the quality of the achieved Ti(C,N), (Ti,Al)N, CrN, TiN coatings based on the resulting X-ray diagrams, collecting by the appliance of the Bragg-Brentano technique (Fig. 9). Because of the overlapping reflections of the substrate and the coating material, as well the relatively small thickness of each layer, difficulties occurred by the identification of the phases. It was also confirmed the presence of reflexes coming from the phases occur in the substrate, e.g. Si, Al, and Al₂Cu (Fig. 9). A very small fraction of other phases present in the substrate material does not allow to realise explicit identification of the observed X-ray spectrum. The presence of substrate reflections was confirmed on every reach X-Ray diffraction collected from the coating due to

the thickness $< 3.5 \mu\text{m}$ of the obtained coatings, which is smaller than the X-ray penetration depth. Using the fixed incidence angle technique (GIXRD method), only reflections from the thin surface layers were collected (Fig. 9).

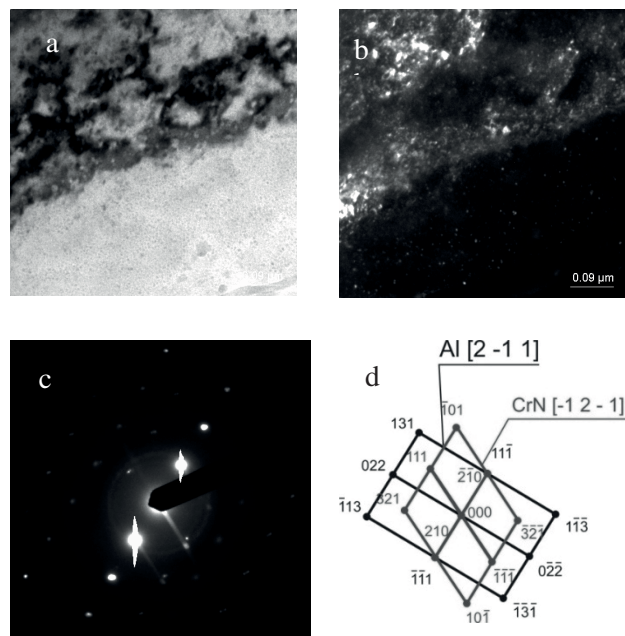


Fig. 10. Structure of the transition zone between the AlSi9Cu substrate and the Cr/CrN/CrN coating: a) bright field, b) dark field, c) diffraction pattern from the area in Figs. 10a and 10b; d) solution of the diffraction pattern from Fig. 10c for the Al phase with the zone axis $[2-11]$ and the CrN phase with zone axis $[-12-1]$. Structure of the Cr/CrN/TiN coating deposited on the AlSi9Cu4 alloy

The TEM investigation results are presented in Figures 10, 11 and 13. For the investigated aluminium alloy, a nanocrystalline microstructure of the CrN surface layer was detected using the dark field TEM technique. The character of the transition zone is visible as a very sharp and rapid change from the substrate phase to the coating layer. For the Cr/CrN/CrN-coated aluminium, the CrN phase was determined (Fig. 10d) as a cubic phase of the $225\text{-Fm}3\text{m}$ space group with $a = b = c = 0.414 \text{ nm}$ of the d-spacing, and the TiN (Fig. 11d) phase was also specified as a cubic phase of the $225\text{-Fm}3\text{m}$ space group with the d-spacing of $a = b = c = 0.424 \text{ nm}$. Moreover, thanks to isomorphology, it was impossible to distinguish the phases TiN and TiAlN using electron diffraction investigations for cases where the titanium atoms were replaced by aluminium atoms: $(\text{Ti,Al})\text{N}$ (Fig. 12d). The polycrystalline character and grain shape of the coatings were identified based on structural

investigations using the TEM dark field method. Also, the electron diffraction patterns confirm the polycrystalline nature of the structure, revealing diffraction circles on the diffraction pattern obtained from the area selected by the SA-aperture (selected area aperture). Based on the structure of the image obtained in the dark, in some cases it was also possible to determine that the average grain size of the investigated coatings was $\leq 20 \text{ nm}$ (Figs. 11b, 12b).

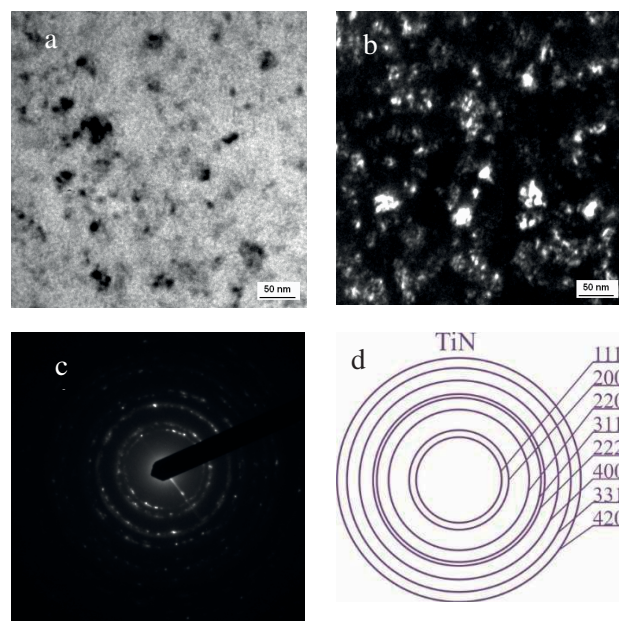


Fig. 11. Structure of the Cr/CrN/TiN coating deposited on the AlSi9Cu4 alloy: a) bright field; b) dark field; c) diffraction pattern from the area in Figs. 11a and 11b; d) solution of the diffraction pattern from Fig. 11c for the TiN phase

As a result of X-ray quantitative and qualitative microanalysis performed by means of the energy dispersive spectrometer, it was possible to confirm the presence of the major alloying elements like Ti, Al, Cr, C, and N as compounds of the obtained coatings Cr/CrN/CrN, Cr/CrN/TiN, and Ti/Ti(C,N)/(Ti,Al)N (Fig. 13).

Concentration changes of the coating component and the substrate material were examined by glow discharge optical spectrometry (GDOS) and the results are presented in Figs. 14 and 15. The tests carried out with GDOS confirmed the occurrence of a transition zone between the coating and substrate material, which results in higher adhesion between the substrate and the coatings. In the transition zone between the substrate and the coatings, the element concentration of the substrate increases,

accompanied by a rapidly decreased concentration of coating elements. The existence of the transition zone should be associated with effects of high-energy ions, causing mixing of the elements in the interface zone. Such results, however, cannot be interpreted explicitly due to the non-homogeneous evaporation of the material from the sample surface. In the case of the investigated coatings, the thin chromium and titanium interlayer, whose role is to increase the adhesion of the main coating to the substrate, can be clearly seen.

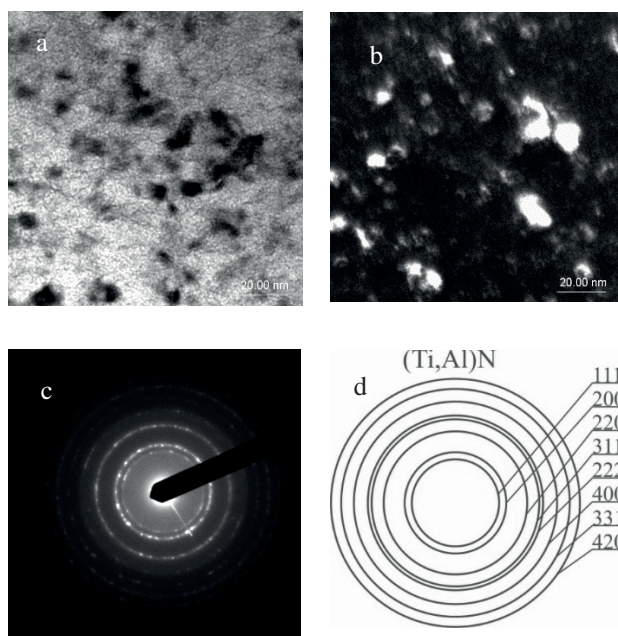


Fig. 12. Structure of the Ti/Ti(C,N)/(Ti,Al)N coating deposited on the AlSi9Cu4 alloy: a) bright field; b) dark field; c) diffraction pattern from the areas in Figs. 12a and 12b; d) solution of the diffraction pattern from Fig. 10k for the (Ti, Al)N phase

The highest value of surface roughness equal to 0.3 mm was measured for the coating of the Ti/Ti(C,N)/(Ti,Al)N type determined probably due to the presence a number of microparticles in the shape of droplets on the substrate (Table 4, Figs. 5,8,13). The found high homogeneity of the Cr/CrN/CrN and Cr/CrN/TiN surface coatings is characterised by a smaller amount of crystallised droplets of liquid metal (Table 4, Figs. 2-4,6), which leads to a lower surface roughness within the range from 0.14 to 0.19 mm. The performed investigations of the surface of the aluminium cast alloys with coated layers partly confirmed a lack of the substrate type effect on the surface roughness (Table 4).

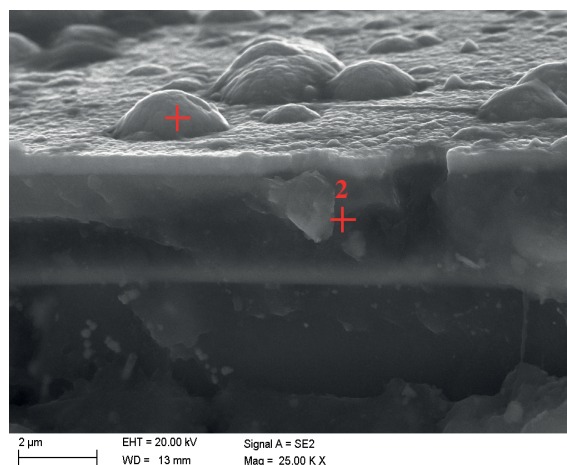


Fig. 13. Fracture of the Ti/Ti(C,N)/(Ti,Al)N coating deposited onto the AlSi9Cu substrate

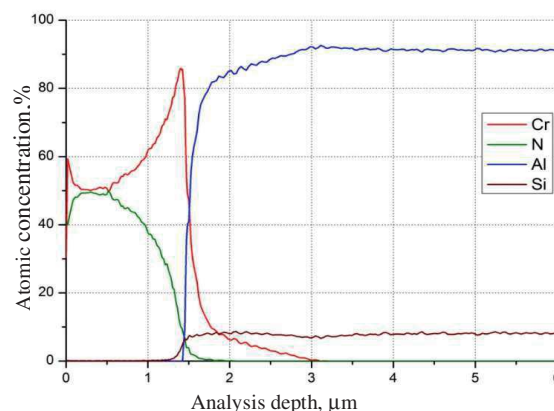


Fig. 14. Changes of constituent concentration of the Cr/CrN/CrN and the AlSi9Cu substrate material

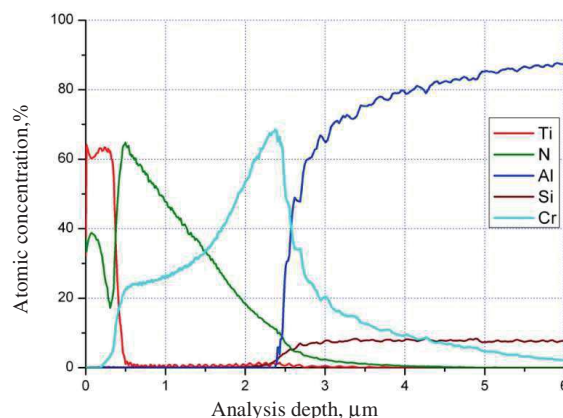


Fig. 15. Changes of constituent concentration of the Cr/CrN/TiN and the AlSi9Cu4 substrate material

Microhardness investigation using the Vickers method revealed that the applied coatings on aluminium alloys substrate allow the plastic deformation resistance of the analysed surfaces to be enhanced effectively (Table 4). The hardness of the uncoated aluminium alloy substrate was 92 HV. In the case of coatings of the Cr/CrN/CrN and Cr/CrN/TiN type produced by the cathodic PVD process in N₂ nitrogen atmosphere, the evident increase in microhardness was found to be above 1900 HV. However, the highest microhardness growth of the surface of above 2000 HV was confirmed for the nitride-carbide coating of the type Ti/Ti(C,N)/(Ti,Al)N obtained in an atmosphere containing CH₄ and N₂ (Table 4).

In order to compare the wear resistance under conditions simulating the real operating conditions of cast aluminium alloys after surface treatment, investigations of the metal-metal system were carried out at a given load of 5 N (Table 4). The wear resistance of the test surfaces was determined on the basis of the friction path performed by the counter specimen until breakthrough of the coating.

Comparing the friction coefficient results with the friction path length, it was found that the best wear resistance was characteristic for materials coated with the Ti/Ti(C,N)/(Ti,Al)N layer. By applying a load of 5 N, the average friction coefficients for the Ti/Ti(C,N)/(Ti,Al)N coating with a sliding rate of 0.05 m/s are in the range of 0.16-0.33, and these values were compared with the other examined coatings' friction coefficient. However, the friction path length results for the Ti/Ti(C,N)/(Ti,Al)N coatings exceeded the results of the friction path length achieved for the Cr/CrN/TiN coatings by as much as 10 times. Due to the small decrease in mass of the sample after the wear test for the investigated Cr/CrN/CrN and Cr/CrN/TiN surfaces, it was not possible to determine the average mass loss. The friction curve has an initial transitional state of an unstabilised way, during which the friction coefficient is reduced together with the increase of sliding distance until the stabilised state is reached, which in the case of the Ti/Ti(C,N)/(Ti,Al)N coating is around 20 m (Figs. 16,17).

Table 3.

The results of quantitative chemical analysis from areas points 1 and 2 on Fig. 11) of the Ti/Ti(C,N)/(Ti,Al)N coating deposited onto the substrate from AlSi9Cu alloy

Chemical elements	The mass and atomic concentration of main elements, %	
	mass	at.
Analysis 1 (point 1)		
N	5.53	14.08
Al	26.93	35.61
Ti	67.54	50.31
Analysis 1 (point 2)		
C	27.26	55.72
N	4.01	7.03
Al	3.72	3.38
Si	1.52	1.33
Ti	63.50	32.55

Table 4.

Summary of results of mechanical properties

Coating	Microhardness, HV	Roughness Ra, µm	Sliding distance, m	Friction coefficient
AlSi9Cu				
Cr/CrN/CrN	1951	0.14	10	0.2-0.3
Cr/CrN/TiN	1929	0.17	5.3	0.13-0.42
Ti/Ti(C,N)/(Ti,Al)N	2159	0.30	52.3	0.16-0.33
AlSi9Cu4				
Cr/CrN/CrN	1960	0.15	18	0.3-0.57
Cr/CrN/TiN	1940	0.19	9.3	0.15-0.26
Ti/Ti(C,N)/(Ti,Al)N	2106	0.29	53.4	0.16-0.32

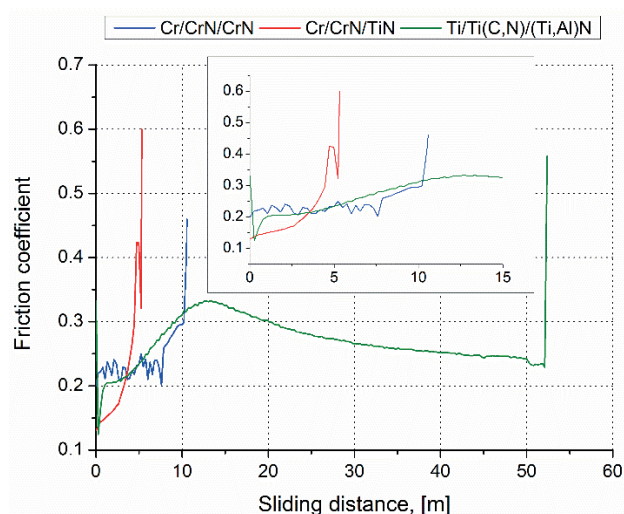


Fig. 16. Dependence of friction coefficient on sliding distance during the wear test for AlSi9Cu1 alloy

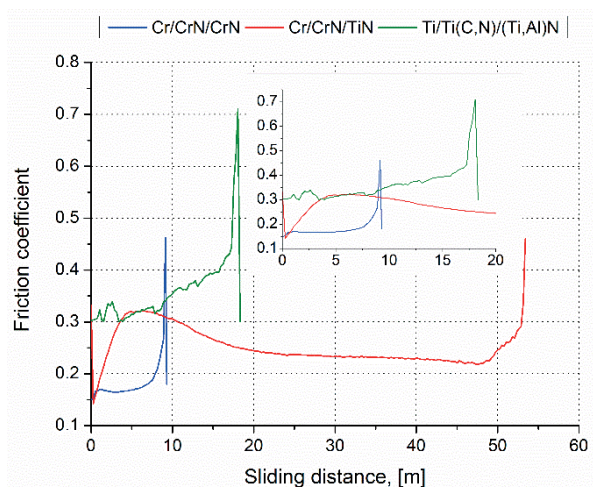


Fig. 17. Dependence of friction coefficient on sliding distance during the wear test for AlSi9Cu4 alloy

4. Conclusions

The investigations presented in this paper reveal that it was possible to successfully deposit coatings on Al-Si-Cu aluminium alloy substrate. In general, the particular findings are as follows:

- Cr/CrN/CrN, Cr/CrN/TiN, and Ti/Ti(C,N)/(Ti,Al)N coatings were deposited successfully on Al-Si-Cu aluminium substrate. The performed SEM investigations of the coatings reveal a microstructure that is tightly adhered to the aluminium substrate

without any visible delamination. The morphology of the surface of the obtained coatings is characterised by a significant inhomogeneity connected with occurrences of multiple drop-shaped particles on the surface.

- The investigation indicates the occurrence of a transition zone between the investigated layers and the substrate material, which affects the improvement of the adhesion.
- Tests carried out using TEM confirmed the polycrystalline nature of the investigated layer and also confirmed that the average grain size of the investigated coatings was ≤ 20 nm based on the structure of the image obtained in the dark field.
- Under the technically dry friction conditions, the friction coefficient for the associations tested is within the range of 0.13-0.57 for the investigated coatings, and it was also confirmed that the best wear resistance is determined for materials coated with a Ti/Ti(C,N)/(Ti,Al)N layer, which are also characterised by the lowest hardness among the investigated coatings.

Further research activity in the field of nanocomposite films and coatings should concentrate on the following problems: development of films with a controlled grain size; increased utilisation of coatings in many types of applications, including in the aerospace and automotive industries; development of hybrid coatings with nanophase biomaterials for biomedical applications; development of new advanced coatings with unique physical and functional properties; and nano-crystallisation of amorphous materials.

References

- [1] M. Avedesian and H. Baker (Eds.), ASM Specialty Handbook: Aluminium and Aluminium Alloys, ASM International, The Materials Information Society, USA, 1999.
- [2] T. Tański, A.D. Dobrzańska-Danikiewicz, K. Labisz, W. Matysiak, Long-term development perspectives of selected groups of engineering materials used in the automotive industry, Archives of Metallurgy and Materials 59/4 (2014) 1729-1740.
- [3] T. Tokarski, Thermo-mechanical processing of rapidly solidified 5083 aluminium alloy - structure and mechanical properties, Archives of Metallurgy and Materials 59/1 (2015) 177-180.
- [4] M.S. Weglowski, S. Dymek, Microstructural modification of cast aluminium alloy AlSi9Mg via friction modified processing, Archives of Metallurgy and Materials 57/1 (2012) 71-78.

- [5] L.A. Dobrzański, M. Krupiński, K. Labisz, B. Krupińska, A. Grajcar, Phases and structure characteristics of the near eutectic Al-Si-Cu alloy using derivative thermo analysis, *Materials Science Forum* 638-642 (2010) 475-480.
- [6] M. Mattox, *Handbook of Physical Vapor Deposition (PVD) Processing*, Elsevier Science, 2010.
- [7] K. Mao, Y. Sun, A. Bloyce, and T. Bell, Surface coating effects on contact stress and wear: an approach of surface engineering design and modelling, *Surface Engineering* 26/1-2 (2010) 142-148.
- [8] M. Pellizzari, High temperature wear and friction behaviour of nitrided, PVD-duplex and CVD coated tool steel against 6082 Al alloy, *Wear* 271 (2011) 2089-2099.
- [9] J. Eriksson, M. Olsson, Tribological testing of commercial CrN, (Ti,Al)N and CrC/C PVD coatings - Evaluation of galling and wear characteristics against different high strength steels, *Surface and Coatings Technology* 205 (2011) 4045-4051.
- [10] I. Endler, M. Höhn, M. Herrmann, H. Holzschuh, R. Pitonak, S. Ruppi, H. van den Berg, H. Westphal, L. Wilde, Aluminum-rich TiAlCN coatings by Low Pressure CVD, *Surface and Coatings Technology* 205 (2010) 1307-1312.
- [11] L.A. Dobrzański, L.W. Żukowska, J. Mikuła, K. Gołombek, D. Pakuła, M. Pancielejko, Structure and mechanical properties of gradient PVD coatings, *Journal of Materials Processing Technology* 201/1-3 (2008) 310-314.
- [12] K. Lukaszewicz, L.A. Dobrzański, G. Kokot, P. Ostachowski, Characterization and properties of PVD coatings applied to extrusion dies, *Vacuum* 86 (2012) 2082-2088.
- [13] K. Lukaszewicz, J. Sondor, K. Balin, J. Kubacki, Characteristics of CrAlSiN + DLC coating deposited by lateral rotating cathode arc PVD and PACVD process, *Applied Surface Science* 312/1 (2014) 126-133.
- [14] M.W. Richert, A. Mazurkiewicz, J.A. Smolik, The deposition of WC-Co coatings by EBPVD technique, *Archives of Metallurgy and Materials* 57/2 (2012) 511-516.
- [15] W. Gębarowski, S. Pietrzyk, Influence of the cathodic pulse on the formation and morphology of oxide coatings on aluminium produced by plasma electrolytic oxidation, *Archives of Metallurgy and Materials* 58/1 (2013) 241-245.
- [16] T. Tański, Characteristics of hard coatings on AZ61 magnesium alloys, *Journal of Mechanical Engineering* 59/3 (2013) 165-174.
- [17] T. Tański, K. Labisz, K. Lukaszewicz, A. Śliwa, K. Gołombek, Characterisation and properties of hybrid coatings deposited onto magnesium alloys, *Surface Engineering* 30/12 (2014) 927-932.
- [18] M. Staszuk, L.A. Dobrzański, T. Tański, W. Kwaśny, M. Muszyńska, The effect of PVD and CVD coating structures on the durability of sintered cutting edges, *Archives of Metallurgy and Materials* 59/1 (2014) 269-274.